Sequential Parametric Optimization for Connected Cruise Control with Application to Fuel Economy Optimization

Nan I. Li, Chaozhe R. He, and Gábor Orosz

Abstract— In this paper, we present a framework for connected cruise control (CCC) design utilizing wireless vehicle-to-vehicle (V2V) communication. We propose a sequential optimization approach to select the control parameters for the available communication links that allows graceful degradation of performance when certain links become unavailable. We apply the theoretical results to improve the fuel economy of a heavy duty vehicle while requiring head-to-tail string stability of the vehicle string. Simulation results are presented to demonstrate the effectiveness of the proposed controller in improving fuel economy.

I. INTRODUCTION

Heavy-duty vehicles (HDVs) account for a significant share of fuel consumption in the transportation sector [1], [2]. Improving the fuel economy of HDVs may save billions of dollars annually in the US only. It has been shown that when the traffic is sparse, previewing geological information (road elevation, wind speed) could lead to significant fuel savings [3], [4]. In dense traffic conditions, the problem becomes much more challenging due to the difficulties in getting reliable information about the surrounding traffic [5]–[8].

In order to monitor the traffic environment in the neighborhood of the vehicle, one may use sensors such as radar, lidar, or camera. However, these can only provide information within the line of sight. To expand the range of sensing, wireless vehicle-to-vehicle (V2V) communication can be used. By appropriately fusing sensory and V2V information, one may reduce traffic congestion [9], [10]. On the other hand, V2V technologies may also be exploited in order to improve the fuel economy of automobiles and HDVs [11]–[13]. Previous works focused on system-level benefits. However, in order to generate "day-one benefits", one may target individual customers. For example, a vehicle may utilize motion information from multiple vehicles ahead to optimize its operation. This so-called connected cruise control (CCC) is different from traditional platooning structures, like cooperative adaptive cruise control (CACC), as it does not require a fixed communication structure or a designated leader [14], [15]. Thus, traffic conditions may be improved even for low penetration of CCC vehicles inserted in the traffic flow of human-driven vehicles [16].

In this paper, we apply CCC to improve the fuel economy of HDVs. In particular, we propose a sequential
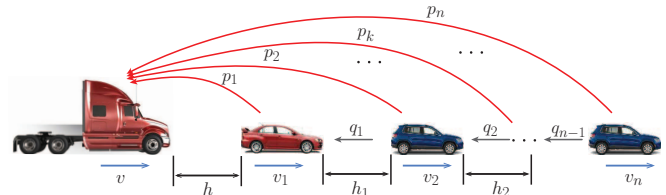
Fig. 1. A string of connected vehicles where the CCC vehicle at the tail receives information from n vehicles ahead. The symbols h, h_i, $i = 1, \ldots, n-1$ denote the headways while $v, v_i, i = 1, \ldots, n$ denote the speed of the vehicles. The symbols p_i, $i = 1, \ldots, n$ denote the control parameters of the CCC vehicle that shall be optimized while q_i, $i = 1, \ldots, n-1$ are the control parameters used by the preceding vehicles and these are assumed to be known.

optimization framework to design the control parameters in the CCC algorithm. This scheme guarantees that when some connections are lost, the system can have a graceful degradation while maintaining head-to-tail string stability (i.e., disturbance attenuation between the vehicle at the head and the vehicle at the tail) of the connected vehicle system. We demonstrate the effectiveness of our algorithm by using case studies.

II. SEQUENTIAL OPTIMIZATION BASED ON COMMUNICATION STRUCTURE

In this section, we present a methodology that can be used to optimize the controller design for a CCC vehicle utilizing V2V information from n vehicles ahead; see Fig. 1. We assume that the preceding vehicles are controlled by human drivers or adaptive cruise control (ACC), i.e., they only react to the motion of the vehicle immediately ahead.

The longitudinal dynamics of the preceding vehicles are described by the car-following model

$$
\begin{aligned}
\dot{h}_i(t) &= v_{i+1}(t) - v_i(t), \\
\dot{v}_i(t) &= g(h_i(t - \xi_i), v_i(t - \xi_i), v_{i+1}(t - \xi_i); q_i),
\end{aligned}
\tag{1}
$$

for $i = 1, ..., n-1$, where the dots denote differentiation with respect to time t, h_i denotes the headway (i.e., the bumper-to-bumper distance) between vehicles i and $i+1$, v_i stands for the speed of vehicle i, and the time delay ξ_i represents the driver reaction time or the sensing delay of the range sensor. The nonlinear function g describes how the driver/controller reacts to the motion of the vehicle ahead, and the vector q_i represents the control parameters, e.g., feedback gains.

The longitudinal dynamics of the CCC vehicle is given by the physics-based model

$$\dot{h}(t) = v_1(t) - v(t), \qquad (2)$$
$$\dot{v}(t) = -f\big(v(t)\big) + u\big(h(t-\sigma), v(t), v(t-\sigma), v_i(t-\sigma); \mathbf{p}_n\big),$$

for $i = 1, ..., n$. Again, h and v denote the headway and velocity, respectively. The term $f\big(v(t)\big)$ collects the physical effects like air resistance, rolling resistance and grade, and assumed to satisfy the following properties:

$$f(v) > 0, \quad \frac{\mathrm{d}f}{\mathrm{d}v} > 0, \quad \frac{\mathrm{d}^2 f}{\mathrm{d}v^2} > 0, \quad \forall\, v > 0, \qquad (3)$$

in order to correspond to the dissipative nature of these effects. Moreover, u represents the designed CCC controller and $\mathbf{p}_n = [p_1, \ldots, p_n]$ collects the control parameters, e.g., feedback gains, related to the vehicles ahead; see Fig. 1. The parameter p_i is associated with the vehicle i and it can be vector valued, while σ stands for the communication delay appearing due to intermittency and packet lost.

To simplify the control design, we assume a particular form of the controller u (that will be specified later). One may complete the design by solving the following parameter optimization problem

$$\begin{aligned} \text{Minimize} \quad & J_n(\mathbf{p}_n), \\ \text{Subject to} \quad & \mathbf{p}_n = [p_1, \ldots, p_n] \in \mathcal{P}_n, \end{aligned} \qquad (4)$$

for $n \in \{1, 2, ..., N\}$. Here n is the index of the farthest vehicle whose motion information is actually used by the CCC vehicle, while N represents the longest link that can be potentially used depending on the V2V broadcast power and the environment. Moreover, J_n is the objective function supposing the vehicle monitors n vehicles ahead, while $\mathcal{P}_n$ denotes the admissible set where $\mathbf{p}_n$ must be chosen from. The corresponding optimizer is denoted by $\mathbf{p}_n^* = [p_1^*, \ldots, p_n^*]$. Here we assume such a solution exists, otherwise the form of the controller u should be redesigned. However, if the connection to the farthest vehicle n is lost, the parameter vector $[p_1^*, \ldots, p_{n-1}^*]$ may not be within the admissible set $\mathcal{P}_{n-1}$ associated with the degraded connected vehicle system. As an example, suppose $\mathcal{P}_n$ is the set such that the string stability of the vehicle system can be satisfied by $\mathbf{p}_n^* \in \mathcal{P}_n$, while $\mathbf{p}_{n-1}^*$ may not make the degraded connected vehicle system string stable.

To avoid this problem and achieve graceful degradation, we propose a sequential optimization scheme for the CCC design and obtain a sub-optimal solution for the parameters, denoted $\mathbf{p}_n^\circ = [p_1^\circ, \ldots, p_n^\circ]$. First, we consider the 2-vehicle string consisting of the CCC vehicle and vehicle 1 immediately ahead and determine the optimizer $\mathbf{p}_1^\circ = p_1^\circ$. Then, we keep this unchanged while adding vehicle 2 to the system and finding the optimal parameter p_2°, that is, $\mathbf{p}_2^\circ = [p_1^\circ, p_2^\circ]$. Thus, we can sequentially build up the vector $\mathbf{p}_n^\circ = [p_1^\circ, \ldots, p_n^\circ]$. Formally, we state the optimization problem as

$$\begin{aligned} \text{Minimize} \quad & J_n(p_n), \\ \text{Subject to} \quad & p_n \in \mathcal{P}_n^\circ, \\ \text{Where} \quad & \mathcal{P}_n^\circ = \{p_n | [p_1^\circ, \ldots, p_{n-1}^\circ, p_n] \in \mathcal{P}_n\}, \\ & n \in \{1, ..., N\}. \end{aligned} \qquad (5)$$

Assumption 1: The sequence of admissible sets $\{\mathcal{P}_n\}_{n=1}^N$ yields that $\forall\, n \in \{1, ..., N\}, \exists\, p_n : [p_1^\circ, \ldots, p_{n-1}^\circ, p_n] \in \mathcal{P}_n$, i.e., $\mathcal{P}_n^\circ \neq \emptyset$.

This assumption is based on the results in [17] where a linear-quadratic optimal control setup provided a state feedback structure, and the control gains were calculated recursively when adding vehicles to the front of the string. It was also shown that this way string stability can be achieved through proper cost function design. This will be treated as a requirement for CCC design in this paper. The results of the sequential optimization performed in Section IV also support Assumption 1.

Our sequential design allows graceful degradation in the following way. If the CCC vehicle loses connection with vehicle k, then by omitting the information received from vehicles $(k + 1), ..., n$, while still utilizing the information received from vehicle $1, ..., (k - 1)$ without changing the corresponding control parameters $p_1^\circ, ..., p_{k-1}^\circ$, the CCC controller can maintain a sub-optimal performance while the constraint $\mathbf{p}_{k-1}^\circ = [p_1^\circ, ..., p_{k-1}^\circ] \in \mathcal{P}_{k-1}$ is satisfied.

III. Problem Formulation Intended for Fuel Saving

In this section, we apply the proposed sequential optimization framework to an $(n + 1)$-vehicle string in order to improve the fuel economy of the CCC vehicle at the tail; see Fig. 1. We start with defining the objective function followed by the definition of the admissible set.

A. Objective function formulation

To optimize the fuel economy of the CCC vehicle, we make the following assumption:

Assumption 2: The fuel consumption rate is proportional to the power requested from the engine

$$P_{\text{eng}} = \begin{cases} P & \text{if} \quad P > 0, \\ 0 & \text{if} \quad P \le 0, \end{cases} \qquad (6)$$

where

$$P = m_{\text{eff}} v\, u = m_{\text{eff}} v\big(\dot{v} + f(v)\big). \qquad (7)$$

Here, P represents the driving power of the CCC vehicle, and $m_{\text{eff}} = m + I/R^2$ is the effective mass of the vehicle, so that m is the vehicle mass, I is the moment of inertia of the rotating elements, and R is the wheel radius.

This assumption neglects some nonlinear effects, e.g, engine idle power, the efficiency difference of engine operation in different operating points, etc. By using more realistic relationships between the power and the fuel rate, one may come up with strategies like the "pulse and glide" in [18], [19] to save fuel, but this is beyond the scope of this paper.

Our goal is to optimize the fuel economy of the CCC vehicle given that the speed profile of the head vehicle n is known. According to Fourier's theory, any periodic function can be represented as an infinite sum of sinusoidal functions, which can also be extended to absolutely integrable non-periodic signals. Hence, we start with optimizing the fuel economy for the speed profile

$$v_n(t) = v^* + \tilde{v}_n(t) = v^* + v_n^{\text{amp}} \sin(\omega t). \qquad (8)$$

To simplify the optimization problem, we linearize (1,2) around the equilibrium

$$h(t) \equiv h^*, \quad h_i(t) \equiv h_i^*, \quad v(t) = v_i(t) \equiv v^*, \quad (9)$$

where h^*, h_i^* and v^* can be obtained using the functions g, f, u in (1,2). The linear system is written in terms of the variables $\tilde{h}(t) = h(t) - h^*$, $\tilde{v}(t) = v(t) - v^*$, $\tilde{h}_i(t) = h_i(t) - h_i^*$, $\tilde{v}_i(t) = v_i(t) - v^*$, $i = 1, ..., n$.

The steady state response to the input (8) becomes

$$v^{\mathrm{ss}}(t) = v^* + \tilde{v}(t) = v^* + v^{\mathrm{amp}}(\omega) \sin\left(\omega t + \phi(\omega)\right), \quad (10)$$

where v^{amp} is the speed fluctuation amplitude of the CCC vehicle, while ϕ is the phase angle compared to the input signal. Both of these are functions of the input frequency ω. In order to derive the output amplitude v^{amp}, one may take the Laplace transform of the linearized system with zero initial conditions and use algebraic manipulations to obtain the head-to-tail transfer function

$$\Gamma_n(s; \mathbf{p}_n) = \frac{\tilde{V}(s)}{\tilde{V}_n(s)}, \quad (11)$$

where $\tilde{V}(s)$ and $\tilde{V}_n(s)$ are the Laplace transform of $\tilde{v}(t)$ and $\tilde{v}_n(t)$, respectively. Notice that in $\Gamma_n(s; \mathbf{p}_n)$, the control parameter $\mathbf{p}_n$ explicitly appears. With the help of the head-to-tail transfer function, one can calculate

$$v^{\mathrm{amp}}(\omega) = |\Gamma_n(\mathrm{i}\omega; \mathbf{p}_n)| v_n^{\mathrm{amp}}. \quad (12)$$

For more details about the derivation see [14].

For one period of the signal (10), one can calculate the work carried out by the engine as

$$W_{\mathrm{eng}} = \int_0^{\frac{2\pi}{\omega}} P_{\mathrm{eng}} \, \mathrm{d}t. \quad (13)$$

The following theorem links this work to the output amplitude v^{amp}.

Theorem 1: At linear-level, the engine work over one period (13) is a monotonic increasing function of the output amplitude (12) .

Proof: Substituting (10) into (6,7), omitting the nonlinear terms, and using (13) yields

$$\frac{W_{\mathrm{eng}}}{m_{\mathrm{eff}}} = \left(v^* f(v^*) + \frac{f'(v^*)}{2}(v^{\mathrm{amp}})^2\right) \frac{2\pi}{\omega}, \quad (14)$$

when no braking is needed ($\forall t \in [0, \frac{2\pi}{\omega}], u(t) \geq 0$) and

$$\frac{W_{\mathrm{eng}}}{m_{\mathrm{eff}}} = \left(v^* f(v^*) + \frac{f'(v^*)}{2}(v^{\mathrm{amp}})^2\right) \frac{\pi}{\omega}$$
$$+ \frac{2v^* f(v^*)}{\Delta \omega}\left(\sqrt{(v^{\mathrm{amp}})^2 - \Delta^2} + \Delta \arcsin\left(\frac{\Delta}{v^{\mathrm{amp}}}\right)\right)$$
$$+ \frac{f'(v^*)}{\omega}\left(\Delta\sqrt{(v^{\mathrm{amp}})^2 - \Delta^2} + (v^{\mathrm{amp}})^2 \arcsin\left(\frac{\Delta}{v^{\mathrm{amp}}}\right)\right), \quad (15)$$

when braking is needed ($\exists t \in [0, \frac{2\pi}{\omega}], u(t) < 0$), where

$$\Delta := \frac{f(v^*)}{\sqrt{\left(f'(v^*)\right)^2 + \omega^2}} < v^{\mathrm{amp}}. \quad (16)$$

Indeed, one can show that in both cases, W_{eng} is monotonically increasing with respect to the amplitude v^{amp}. ∎

According to Theorem 1 and (12), minimizing the fuel consumption is equivalent to finding parameter $\mathbf{p}_n$ that minimizes $|\Gamma_n(\mathrm{i}\omega; \mathbf{p}_n)|$. That is, the objective function of the optimization for the sinusoidal speed profile (8) can be designed as

$$\hat{J}_n(\omega; \mathbf{p}_n) = |\Gamma_n(\mathrm{i}\omega; \mathbf{p}_n)|. \quad (17)$$

In order to generalize the arguments above for a general fluctuation $\tilde{v}_n(t)$, we take the Fourier transform of $\tilde{v}_n(t)$ to obtain its frequency component distribution $w(\omega)$. Then we construct the objective function

$$J_n(\mathbf{p}_n) = \int_0^\infty w(\omega)|\Gamma_n(\mathrm{i}\omega; \mathbf{p}_n)| \mathrm{d}\omega, \quad (18)$$

that is used in (4) or (5).

B. Admissible set

When solving the constrained optimization problems (4) or (5), we need to define the admissible sets $\mathcal{P}_n$ and $\mathcal{P}_n^\circ$, $n \in \{1, ..., N\}$. In this paper, we require head-to-tail string stability, that is, we require that the speed fluctuations of the head vehicle are attenuated by the CCC vehicle at the tail. By using Fourier components (cf. (8)), one may formulate the condition for string stability as

$$\frac{v^{\mathrm{amp}}(\omega)}{v_n^{\mathrm{amp}}} = |\Gamma_n(\mathrm{i}\omega; \mathbf{p}_n)| < 1, \quad \forall \omega > 0, \quad (19)$$

(cf. (12)).

Thereafter, the objective function and the admissible sets can be specified and computed, and used for control parameter optimization for fuel efficient CCC design. The solutions for (5) shall improve the fuel economy of the CCC vehicle and enforce the head-to-tail string stability condition of the connected vehicle system even with changing connectivity.

IV. CASE STUDIES

In this section, we consider a certain form of CCC design and use the method proposed above to optimize its control parameters.

We start with specifying the car following model (1). In particular, we consider identical drivers modeled by

$$\dot{h}_i(t) = v_{i+1}(t) - v_i(t),$$
$$\dot{v}_i(t) = \alpha_{\mathrm{h}}\left(V(h_i(t - \xi_{\mathrm{h}})) - v_i(t - \xi_{\mathrm{h}})\right) \quad (20)$$
$$+ \beta_{\mathrm{h}}(v_{i+1}(t - \xi_{\mathrm{h}}) - v_i(t - \xi_{\mathrm{h}})),$$

for $i = 1, ..., n - 1$. Here, α_{h} and β_{h} are the control gains used by the human drivers, while ξ_{h} represents the human reaction time. The range policy function

$$V(h) = \begin{cases} 0 & \text{if} \quad h \leq h_{\mathrm{st}}, \\ \frac{v_{\max}}{2}\left[1 - \cos\left(\pi\frac{h - h_{\mathrm{st}}}{h_{\mathrm{go}} - h_{\mathrm{st}}}\right)\right] & \text{if} \quad h_{\mathrm{st}} < h < h_{\mathrm{go}}, \\ v_{\max} & \text{if} \quad h \geq h_{\mathrm{go}}, \end{cases} \quad (21)$$

describes the desired speed of the driver as a function of the headway. For small headway $h < h_{\mathrm{st}}$, the vehicle intends to stop; for large headway $h > h_{\mathrm{go}}$, it intends to travel with

the maximum speed $v_{\max}$; between h_{st} and h_{go}, the desired speed increases monotonically with the headway. In this paper we set $h_{st} = 10[m]$, $h_{go} = 40[m]$, $v_{\max} = 30[m/s]$, $\xi_h = 0.45[s]$, $\alpha_h = 0.6[1/s]$, $\beta_h = 0.9[1/s]$; see [20].

The CCC vehicle is assumed to be a HDV and its longitudinal dynamics is given based on the physics-based model

$$m_{eff}\dot{v} = mg\sin\phi + \gamma mg\cos\phi + \kappa(v + v_w)^2 + \frac{\eta T_e + T_b}{R},$$
(22)

see [12], [21]. Here, g is the gravitational constant, ϕ is the inclination angle, γ is the rolling resistance coefficient, κ is the air drag constant, v_w is the speed of the headwind, η is the gear ratio (that includes the final drive ratio and the transmission efficiency), and T_e is the engine torque, and T_b is the axle braking torque. The parameter values used in this paper can be found in [4], and these are based on a Prostar truck, a class 8 HDV manufactured by Navistar. For more details of the HDV simulation, see [22].

For simplicity, we neglect the headwind and grade. Thus, the longitudinal dynamics (2) is given by

$$\dot{h}(t) = v_1(t) - v(t),$$
$$\dot{v}(t) = -f(v(t)) + u(t) = -(a + cv^2(t)) + u(t),$$
(23)

where

$$a = \frac{\gamma m g}{m_{eff}}, \quad c = \frac{\kappa}{m_{eff}}, \quad u = \frac{\eta T_e + T_b}{m_{eff} R}. \quad (24)$$

The CCC controller to be optimized is assumed to take the form

$$u(t) = \alpha\big(V(h(t-\sigma)) - v(t-\sigma)\big)$$
$$+ \sum_{i=1}^{n} \beta_i\big(v_i(t-\sigma) - v(t-\sigma)\big) + f(v(t)), \quad (25)$$

where the term $f(v(t))$ is added to cancel the rolling resistance and air resistance. We remark that this may also be achieved by using integral action [23]. Note that the other terms in controller resemble the terms in (20) with the same range policy (21), but with the delay $\sigma = 0.15[s]$ resulted by intermittency in communication and digital control.

The system (20,23,25) possesses the uniform flow equilibrium

$$h(t) = h_i(t) \equiv h^*, \quad v(t) = v_i(t) \equiv v^* = V(h^*), \quad (26)$$

for $i = 1, ..., n$; cf. (9). Linearizing the system about this equilibrium we obtain

$$\dot{\tilde{h}}_i(t) = \tilde{v}_{i+1}(t) - \tilde{v}_i(t),$$
$$\dot{\tilde{v}}_i(t) = \alpha_h\big(N^*\tilde{h}_i(t-\xi_h) - \tilde{v}_i(t-\xi_h)\big)$$
$$\quad + \beta_h\big(\tilde{v}_{i+1}(t-\xi_h) - \tilde{v}_i(t-\xi_h)\big),$$
$$\dot{\tilde{h}}(t) = \tilde{v}_1(t) - \tilde{v}(t),$$
$$\dot{\tilde{v}}(t) = \alpha\big(N^*\tilde{h}(t-\sigma) - \tilde{v}(t-\sigma)\big)$$
$$\quad + \sum_{i=1}^{n} \beta_i\big(\tilde{v}_i(t-\sigma) - \tilde{v}(t-\sigma)\big),$$
(27)

for $i = 1, ..., n-1$, where $N^* = V'(h^*)$ is the derivative of $V(h)$ at h^*.

The head-to-tail transfer function is given by

$$\Gamma_n(s; \mathbf{p}_n) = \frac{\alpha N^*\big(T_h(s)\big)^{n-1} + s\sum_{i=1}^{n} \beta_i\big(T_h(s)\big)^{n-i}}{s^2 e^{\sigma s} + \big(\alpha + \sum_{i=1}^{n} \beta_i\big)s + \alpha N^*},$$
(28)

where

$$T_h = \frac{\beta_h s + \alpha_h N^*}{s^2 e^{\xi_h s} + (\alpha_h + \beta_h)s + \alpha_h N^*}, \quad (29)$$

see [14]. Now we present two case studies and their optimization results.

A. 2-vehicle string

In this subsection we consider a scenario when the CCC vehicle only monitors the motion of the vehicle immediately ahead; see Fig. 2(a).

First, we assign the sinusoidal speed profile $v_1(t) = 15 + 0.5\sin(t)[m/s]$ to the head vehicle. In Fig. 2(b), the contours of the objective function

$$\hat{J}_1(\omega; \alpha, \beta_1) = |\Gamma_1(i\omega; \alpha, \beta_1)|$$
$$= \left|\frac{\beta_1 i\omega + \alpha N^*}{-\omega^2 e^{i\omega\sigma} + (\alpha + \beta_1)i\omega + \alpha N^*}\right|, \quad (30)$$

(cf. (17,28)) are plotted for $\omega = 1[rad/s]$ and $\sigma = 0.15$ [s] in the (β_1, α)-plane. The light blue area enclosed by the black solid curve is the string stable region where $|\Gamma_1(i\omega; \alpha, \beta_1)| < 1$ for all $\omega > 0$. This domain corresponds to the admissible set $\mathcal{P}_1 = \mathcal{P}_1^\circ$. The parameter combination for the optimal design is marked by point E. The corresponding time profiles are shown in Fig. 2(d). Note that simulations are ran using the nonlinear system (20,21,23,24,25), and include fuel consumption map given in [22] and the gear change map given in [24]. Consequently, the true optimal parameters may slightly differ from those corresponding to point E that is based on the linear system (27), which is the linearization of (20,21,23,24,25) about the equilibrium $v^* = 15[m/s]$. Four additional parameter combinations are marked as A–D and the corresponding fuel consumption results measured in miles per gallon (MPG) are summarized in Table 1. Notice that although the parameters corresponding to point A and D provide better fuel economy than those of the point E, they are outside of the admissible string stable domain.

Similarly, we depict the contours of

$$J_1(\alpha, \beta_1) = \int_0^\infty w(\omega)\hat{J}_1(\omega; \alpha, \beta_1)d\omega, \quad (31)$$

in Fig. 2(c) corresponding to the speed profile shown in Fig. 2(e). This profile is obtained from the Ann Arbor Safety Pilot Experiment [25]. Notice that the optimal parameter combination (marked by point J) differs significantly from the single frequency case (marked by point E in Fig. 2(b)). Again, the fuel consumption results are summarized in Table 2, corresponding to the points marked by F–J in Fig. 2(c).
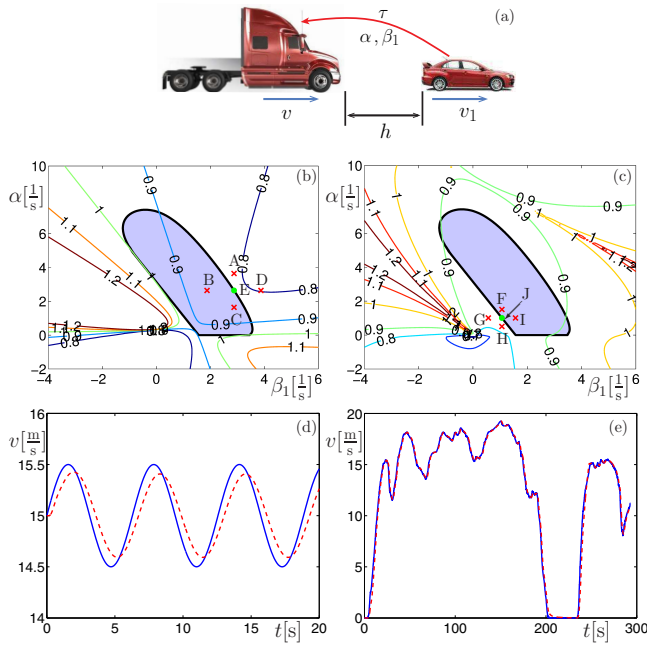
Fig. 2. (a) The layout of a 2-vehicle string. (b)(c) The contours of the objective functions corresponding to the speed profiles shown in panels (d)(e). The light blue areas enclosed by the black solid curves represent the string stable region. (d)(e) Speed profiles of the vehicles: blue solid curves correspond to the head vehicle, while red dashed curves correspond to the CCC vehicle.

	$(\alpha, \beta_1)[1/s]$	MPG	
Point A	(3.65,2.85)	7.6425	String Unstable
Point B	(2.65,1.85)	7.3887	String Stable
Point C	(1.65,2.85)	7.5414	String Stable
Point D	(2.65,3.85)	7.7410	String Unstable
Point E	(2.65,2.85)	7.6414	Optimal point

TABLE I

FUEL CONSUMPTION RESULTS CORRESPONDING TO FIG. 2(B).

	$(\alpha, \beta_1)[1/s]$	MPG	
Point F	(1.50,1.05)	6.1968	String Stable
Point G	(1.00,0.55)	6.0578	String Unstable
Point H	(0.50,1.05)	6.2156	String Unstable
Point I	(1.00,1.55)	6.1916	String Stable
Point J	(1.00,1.05)	6.2143	Optimal point

TABLE II

FUEL CONSUMPTION RESULTS CORRESPONDING TO FIG. 2(C).

B. 3-vehicle string

We now consider a scenario when the CCC vehicle monitors two vehicles ahead; see Fig. 3(a). Then we optimize the control parameters $(\alpha, \beta_1, \beta_2)$ of the CCC vehicle using the proposed sequential optimization scheme. That is, the CCC vehicle inherits the optimal design for α and β_1 derived in the previous subsection, and then we search for the optimal β_2.

Again, we first assign the sinusoidal speed profile $v_2(t) = 15 + 0.5\sin(t)$[m/s] for the head vehicle. The values of the
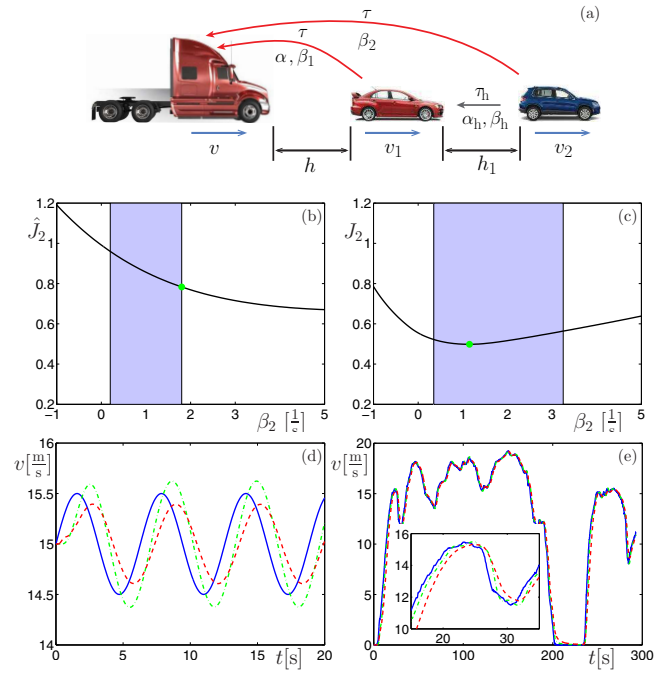

Fig. 3. (a) The layout of a 3-vehicle string. (b)(c) The values of the objective functions corresponding to the speed profiles shown in panels (d)(e). The blue shaded areas highlight the range for string stability. (d)(e) Speed profiles of the vehicles: blue solid curves correspond to the head vehicle, green dashed curves correspond to the middle vehicle, while red dashed curves correspond to the CCC vehicle.

$\beta_2[1/s]$	MPG	
0.00	6.5134	String Unstable
1.00	7.3190	String Stable
1.50	7.6474	String Stable
1.70	7.7642	String Stable
1.80	7.8196	Optimal Point
2.00	7.9247	String Unstable

TABLE III

FUEL CONSUMPTION RESULTS CORRESPONDING TO FIG. 3(B).

$\beta_2[1/s]$	MPG	
0.00	5.9421	String Unstable
0.50	6.2887	String Stable
1.00	6.3750	String Stable
1.15	6.3847	Optimal point
1.50	6.3856	String Stable
2.00	6.3459	String Stable

TABLE IV

FUEL CONSUMPTION RESULTS CORRESPONDING TO FIG. 3(C).

objective function

$$\hat{J}_2(\omega; \beta_2) = |\Gamma_2(i\omega; \beta_2)|$$
$$= \left| \frac{(\beta_1 i\omega + \alpha N^*)\dfrac{\beta_h i\omega + \alpha_h N^*}{-\omega^2 e^{i\omega\xi_h} + (\alpha_h + \beta_h)i\omega + \alpha_h N^*} + \beta_2 i\omega}{-\omega^2 e^{i\omega\sigma} + (\alpha + \beta_1 + \beta_2)i\omega + \alpha N^*} \right|,$$

(32)

(cf. (17,28)) are plotted in Fig. 3(b) for $\omega = 1$[rad/s] and $\sigma = 0.15$[s]. The blue shaded area indicates string stability for

the control parameter β_2. This corresponds to the admissible set $\mathcal{P}_2^\circ$. The parameter for the optimal design is marked by the green dot and the corresponding time profiles are shown in Fig. 3(d). The fuel consumption results corresponding to different β_2 values are summarized in Table III. Again, these are generated by using the system model (20,21,23,24,25) with realistic fuel consumption and gear change map [22], [24].

For the realistic speed profile shown in Fig. 3(e), the values of the objective function

$$J_2(\beta_2) = \int_0^\infty w(\omega)\hat{J}_2(\omega;\beta_2)\mathrm{d}\omega \tag{33}$$

are shown in Fig. 3(c) for different β_2 values. The corresponding fuel consumption results are summarized in Table IV. Notice that for $\beta = 1.5[1/s]$, the CCC vehicle actually has slightly better fuel economy over the claimed optimal design at $\beta = 1.15[1/s]$. In order to understand this discrepancy, notice that within the interval $[0.5\ 1.5]$ the J_2 curve is quite flat. In this situation, the nonlinearities in (20,21,23,24,25) can shift the optimal parameters. Still, the MPG from our suggested design is very close to the best MPG.

To sum up, by simulations we justified that the MPG values match well with the contours of the objective functions. The optimal design led to MPG values that are optimal or very close to optimal.

V. CONCLUSION AND FUTURE WORK

In this paper we proposed a sequential optimization framework for connected cruise control design, which exploits information from multiple vehicles ahead. Case studies demonstrated the effectiveness of the proposed CCC controller in improving fuel economy of individual vehicles as well as in smoothing traffic flow by enforcing the head-to-tail string stability. In future work, we will to apply the proposed optimization framework on more flexible and time varying communication structures, and compare our parameter optimization scheme to other optimization approaches.

VI. ACKNOWLEDGMENTS

REFERENCES

[1] S. C. Davis, S. W. Diegel, and R. G. Boundy, "Transportation energy data book: Edition 32," U.S. Department of Energy, Tech. Rep., 2013.

[2] U.S. Department of Transportation, "2012 commodity flow survey united states," Tech. Rep., 2014.

[3] A. Sciarretta, G. De Nunzio, and L. Ojeda, "Optimal ecodriving control: Energy-efficient driving of road vehicles as an optimal control problem," *IEEE Control Systems Magazine*, vol. 35, no. 5, pp. 71–90, Oct 2015.

[4] C. R. He, H. Maurer, and G. Orosz, "Fuel consumption optimization of heavy-duty vehicles with grade, wind, and traffic information," *Journal of Computational and Nonlinear Dynamics*, vol. 11, no. 6, p. 061011, 2016.

[5] N. Kohut, K. Hedrick, and F. Borrelli, "Integrating traffic data and model predictive control to improve fuel economy," in *12th IFAC Symposium on Control in Transportation Systems*, 2009, pp. 155–160.

[6] S. E. Li, Z. Jia, K. Li, and B. Cheng, "Fast online computation of a model predictive controller and its application to fuel economy–oriented adaptive cruise control," *IEEE Transactions on Intelligent Transportation Systems*, vol. 16, no. 3, pp. 1199–1209, 2015.

[7] I. V. Kolmanovsky and D. Filev, "Terrain and traffic optimized vehicle speed control," in *Advances in Automotive Control*, 2010, pp. 378–383.

[8] K. K. McDonough, "Developments in stochastic fuel efficient cruise control and constrained control with applications to aircraft," Ph.D. dissertation, University of Michigan, 2015.

[9] S. S. Avedisov and G. Orosz, "Nonlinear network modes in cyclic systems with applications to connected vehicles," *Journal of Nonlinear Science*, vol. 25, no. 4, pp. 1015–1049, 2015.

[10] M. Wang, W. Daamen, S. P. Hoogendoorn, and B. van Arem, "Cooperative car-following control: Distributed algorithm and impact on moving jam features," *IEEE Transactions on Intelligent Transportation Systems*, vol. 17, no. 5, pp. 1459–1471, 2016.

[11] E. Van Nunen, R. J. A. E. Kwakkernaat, J. Ploeg, and B. D. Netten, "Cooperative competition for future mobility," *IEEE Transactions on Intelligent Transportation Systems*, vol. 13, no. 3, pp. 1018–1025, 2012.

[12] A. Alam, "Fuel-efficient heavy duty vehicle platooning," Ph.D. dissertation, Kungliga Tekniska Högskolan, 2014.

[13] M. S. Kamal, J. Imura, T. Hayakawa, A. Ohata, and K. Aihara, "Smart driving of a vehicle using model predictive control for improving traffic flow," *IEEE Transactions on Intelligent Transportation Systems*, vol. 15, no. 2, pp. 878–888, 2014.

[14] L. Zhang and G. Orosz, "Motif-based design for connected vehicle systems in presence of heterogeneous connectivity structures and time delays," *IEEE Transactions on Intelligent Transportation Systems*, vol. 17, no. 6, pp. 1638–1651, 2016.

[15] J. I. Ge and G. Orosz, "Optimal control of connected vehicle systems with communication delay and driver reaction time," *IEEE Transactions on Intelligent Transportation Systems (under review)*.

[16] N. I. Li and G. Orosz, "Dynamics of heterogeneous connected vehicle systems," in *Proceedings of the 13th IFAC Workshop on Time Delay Systems*. IFAC-PapersOnLine, 2016, pp. 171–176.

[17] J. I. Ge and G. Orosz, "Optimized connected cruise control with time delay." IFAC-PapersOnLine, 2015, pp. 468–473.

[18] S. E. Li, H. Peng, K. Li, and J. Wang, "Minimum fuel control strategy in automated car-following scenarios," *IEEE Transactions on Vehicular Technology*, vol. 61, no. 3, pp. 998–1007, 2012.

[19] S. E. Li, K. Deng, Y. Zheng, and H. Peng, "Effect of pulse-and-glide strategy on traffic flow for a platoon of mixed automated and manually driven vehicles," *Computer-Aided Civil and Infrastructure Engineering*, vol. 30, no. 11, pp. 892–905, 2015.

[20] J. I. Ge and G. Orosz, "Dynamics of connected vehicle systems with delayed acceleration feedback," *Transportation Research Part C*, vol. 46, pp. 46–64, 2014.

[21] G. Orosz and S. P. Shah, "A nonlinear modeling framework for autonomous cruise control," in *Proceedings of the ASME Dynamic Systems and Control Conference*, pp. 467–471.

[22] C. R. He, W. B. Qin, N. Ozay, and G. Orosz, "Hybrid system based analytical approach for optimal gear shifting schedule design," in *Proceedings of the ASME Dynamic Systems and Control Conference*, 2015, pp. V003T41A003–V003T41A003.

[23] G. Orosz, "Connected cruise control: modeling, delay effects, and nonlinear behavior," *Vehicle System Dynamics*, vol. 54, no. 8, pp. 1147–1176, 2016.

[24] L. Zhang, C. He, J. Sun, and G. Orosz, "Hierarchical design for connected cruise control," in *ASME 2015 Dynamic Systems and Control Conference*. American Society of Mechanical Engineers, 2015, pp. V001T17A005–V001T17A005.

[25] UMTRI. (2012) Safety pilot model deployment. [Online]. Available: http://safetypilot.umtri.umich.edu/index.php?content=about